HASIL CEK9_60010383

by 60010383 Anton Yudhana

Sensing and Bio-Sensing Research 34 (2021) 100461

Contents lists available at ScienceDirect

Sensing and Bio-Sensing Research

journal homepage: www.elsevier.com/locate/sbsr

Multi sensor application-based for measuring the quality of human urine on first-void urine

Anton Yudhana [a,*], Subhas Mukhopadhyay [b], Oky Dicky Ardiansyah Prima [c], Son Ali Akbar [a], Fatma Nuraisyah [d], Ilham Mufandi [e], Khoirul Hafizh Fauzi [a], Nurul Ainun Nasyah [a]

[a] Department of Electrical Engineeirng, Faculty of Technology Industry, Universitas Ahmad Dahlan, Unit IV, Jl. Ringroad Selatan, Kragilan, Tamanan, Banguntapan, Bantul, Special Region of Yogyakarta 55191, Indonesia
[b] Faculty of Science and Engineering, Macquarie University, Sydney, NSW 2109, Australia
[c] Graduate School of Software and Information Science, Iwate Prefectural University, Takizawa, Japan
[d] Fakultas Kesehatan Masyarakat, Universitas Ahmad Dahlan, Indonesia
[e] Department of Chemical Engineering, Indian Institute of Technology Delhi, New Delhi 110016, India

ARTICLE INFO

Keywords:
Ammonia
Invasive
pH Urine
Sensor
Turbidity
and Urine detection

ABSTRACT

Urine can be used to diagnose diabetes in a non-invasively manner. Examination of blood sugar levels as an indicator of diabetics is currently carried out using invasive methods. However, most people are not comfortable with the invasive methods used. Early diagnosis of diabetics using non-invasive methods is very important to continue to be developed, including by checking the quality of the urine. This study aims to create a quality urine detection based on urine pH, turbidity, and ammonia concentration by using multi-sensor: pH4502C to measure pH level, SEN0189 to measure urine turbidity, and MQ137 to measure ammonia concentration. Urine samples of 15 subjects were collected early in the morning before doing any activities. For the experiment, all sensors can be read analog signals which are received by an Arduino Nano as a micro-controller and converted into digital values in the form of pH scale, Nephelometric Turbidity Units (NTU), and parts per million (ppm). These values are displayed on the LCD display. Theexperiments showed that the measured sensor using the system was compared with the calculated sensor from a manual calculation using an equation. These comparisons were used to know the error percentage. The average value of urine measurement from 15 subjects obtained pH urine of 5.62, turbidity urine of 0.59 NTU, and ammonia urine of 0.66 ppm. The accuracy percentages of pH sensor, ammonia sensor, and turbidity sensor are 97.69%, 98.32%, and 97.09%. All sensors were proved capable to measure the quality of human urine. The results of this study became the basis for the initial diagnosis of diabetes from the quality of the urine using non invasive method.

1. Introduction

The human body has three metabolic waste removal system, such as excretion, secretion, and defection [1]. The excretory system process and disposes of metabolic wastes that are not used by the body. This system has the ability to remove toxins from the body. Excretory system consists of the kidneys, liver, lungs, and skin. Urine is a metabolic product, which is excreted by the kidneys through the process of urination. For the human body, the excretion system is important to eliminate of the residual molecules filtered by the kidneys and to maintain the hemostasis of body fluids. Before being excreted through the urethra, urine first filtered by the kidneys and stored in the urinary bladder. Human produces 1.5 to 2 l of urine per day [2]. Urine contains various types of substances, such as urea, ammonia, protein breakdown residues, excess substances in the blood, and urine acids [3,4]. Therefore, urine needs to be eliminated from the body so that it does as not harm our health.

Urine quality can be characterized by color, clarity, and odor. Urine color is affected by fluids and drinks consumed by the body [5,6]. Bright and clear urine color indicates that the body has consumed adequate amount of fluids, on the contrary, cloudy urine indicates that the body is dehydrated and lacks fluids [7]. The urine odor is affected by the ammonia content [8]. The high ammonia level is caused by lack of fluids in the body [9]. The increase in ammonia concentration in urine

* Corresponding author.
E-mail address: eyudhana@ee.uad.ac.id (A. Yudhana).

https://doi.org/10.1016/j.sbsr.2021.100461
Received 3 September 2021; Received in revised form 18 October 2021; Accepted 21 October 2021
Available online 30 October 2021

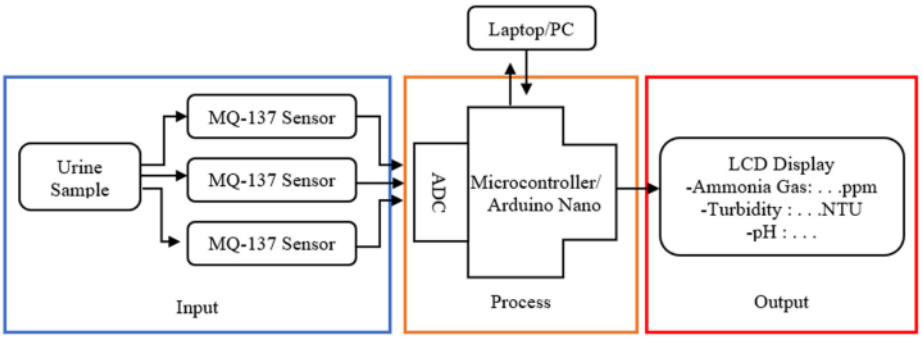

Fig. 1. Functional block diagram of system hardware.

increase is caused by the hydrolysis of urea into ammonia (NH_3), ammonium, and ion carbonate (CO_3^{2-}) [10,11]. A low ammonia concentration in the urine is a sign of a positive acid balance compared to the bicarbonate concentration [12]. In addition, the quality of urine will change due to the effects of bacterial growth. Urine becomes cloudy if left for a long time because it is contaminated with bacteria. Urinary bladder infections can cause odor and cloudiness of urine [13,14].

In medicine, urine is used to diagnose diseases, such as colorectal cancer [15], diabetes mellitus [16], pregnancy complications [17], and to determine various kidney diseases such as: (Glomerulonephritis, nephrotic syndrome, and pyelonephritis) [18]. Typically, diabetes mellitus is diagnosed using an invasive method that involves pricking the skin to draw blood [19], However, the invasive test requires high costs and a long testing time. Other diabetes test include the fasting blood sugar test [20], glucose tolerance test [21], Hemoglobin A1C test (HbA1c) [22], radioactive iodine uptake test [23], serum glucose test [24], thyroid test echo-diagram, thyroid function test [25], and GC/MS based metabolic approach [26]. However, these tests are also expensive and it takes a long time to get the results.

Previous studies have shown that urine can be used as an alternative solution to solve testing problem in diabetic patients [27–30]. According to [31], diabetes is a metabolic disorder caused by the function of the pancreas not being able to produce enough insulin for the body or not being able to utilize the insulin produced effectively. There are two types of diabetes, type 1 and type 2 diabetes, which cause high blood glucose levels and can cause abnormal body conditions [32]. Glucose cannot enter the cells of diabetic patients. As a result, the pancreas cannot produce insulin and the liver will break down rapidly to meet glucose [33–35].

There are three methods to examine urine in the body, namely macroscopic, microscopic [36,37] and urine chemistry checkup [38]. Analysis of erythrocytes, epithelial cells, Red Blood Cells (RBC), White Blood Cells (WBC) bacteria, crystals, parasites, and leukocytes using microscopic methods [39,40]. The microscopic method examines the

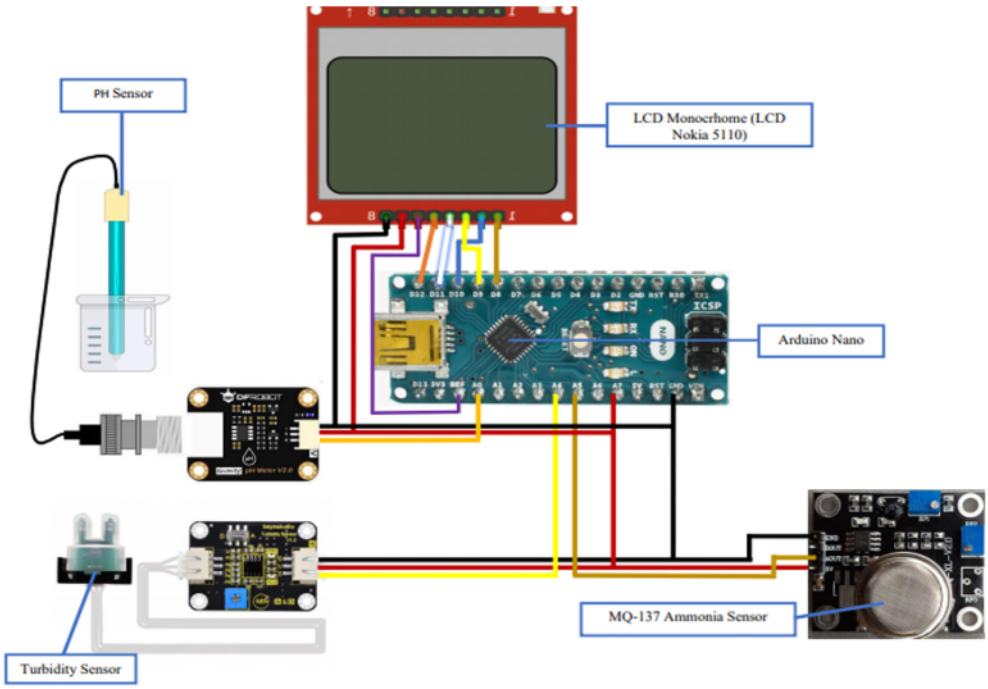

Fig. 2. Electronic circuit of proposed system.

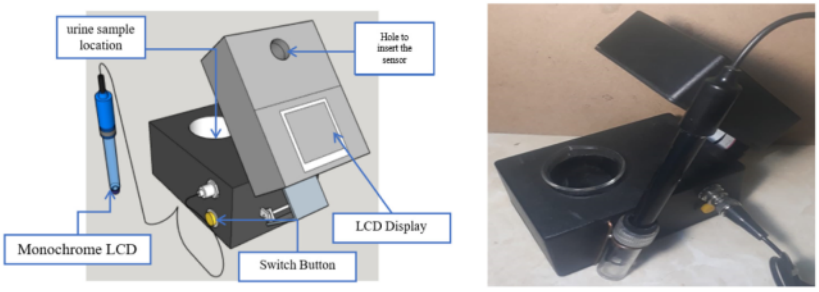

a) 3D digital design b) Implementation of the actual system

Fig. 3. Prototype of the proposed system.

color, clarity, odor, and pH of urine. Urine chemistry checkup tests for glucose, ketones, blood, bilirubin, protein, urobilinogen, nitrite, and leukocyte esterase. The urine of diabetics contains excess glucose, which is excreted in the urine.

Non-invasive urine testing can be achieved by using smart sensors [41,42]. The motivation to detect diabetes in a non-invasive method is easy operation, high sensitive, not expensive, and real-time testing [43,44]. Urine can be used as new biomarkers in early detection of non-invasive diseases [45]. Several studies have reported research in the field of urine as a new biomarker for non-invasive detection of diabetes mellitus. [46] reported non-invasive detection framework for diabetic complication through image processing and pattern analysis of facial color. The detection of macroalbuminuria using urine has been reported in [47,48]. Research result from [49] detected the diabetes mellitus by facial block color with a sparse representation classifier. [50] conducted the experiment to detect urea in urine using an electrochemical sensor. [30] reviewed non-invasive detection for diabetes mellitus advance in biosensors will be available in the future to detect diseases [51,52]. Biosensors also can be used for bacteria detection in urine [53,54]. Non-invasive detection of urine by using smart toilet systems were introduced by [55–57]. A non-invasive detection of heart rate by using sensor was introduced by [58]. The non-invasive detection also was used for

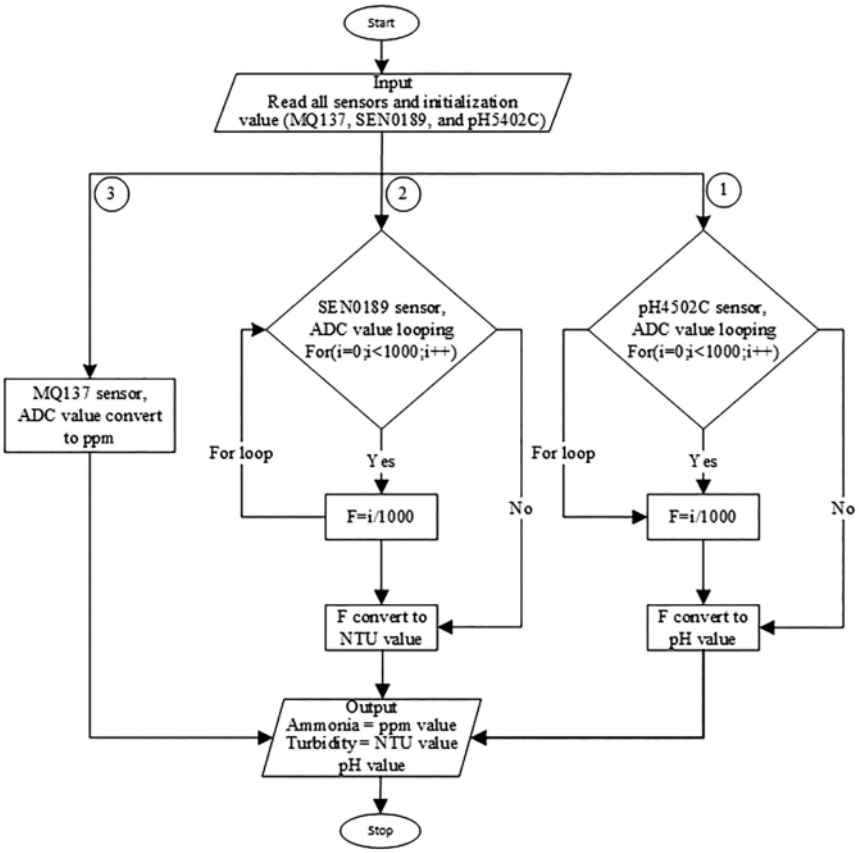

Fig. 4. The flowchart of multi sensor including pH sensor, turbidity sensor, and ammonia sensor.

```
// Initialization LCD
#include "U8glib.h"  // Include U8glib library
U8GLIB_PCD8544 u8g(13, 11, 10, 9, 8);
int Variable1;
```

Fig. 5. An initialization pin in LCD.

liver detection using smart sensors [59], monitoring of sweet glucose in urine [60], creatinine levels [61,62], point-of-care monitoring of kidneys [63], and real-life application diagnostics [64]. In other fields, smart sensors can be used for monitoring in agriculture field to improve the production [65], modification of manual raindrop [66], human emotion as physiological field [67], monitoring devices to care for the elderly [68].

The purpose of this study is to create a urine quality detector consisting of pH, turbidity, and ammonia concentration using multi sensor. This study was carried out non-inventively by collecting urine samples from 15 healthy subjects. The sensors consisted of: pH4502C to measure pH level, SEN0189to measure urine turbid, and MQ137 to measure ammonia concentration. The analog signals in urine are measured by sensors and sent to the Arduino Nano microcontroller converted into digital values in the form of pH scale, Nephelometric Turbidity Units (NTU), and parts per million (ppm). All results can be displayed on the LCD display.

2. Materials and methods

2.1. Hardware design

Fig. 1 shows the hardware design in this research. Three sensors were connected to a sample urine including pH sensor, turbidity sensor, and ammonia sensor. These sensors are controlled by the Arduino Nano and the measurements are sent to LCD display (Nokia 5010). Output data from three sensors are in the form of digital value with the numeric of pH measurement value, Nephelometric Turbidity Unit (NTU), and Part Per Million (ppm). This design makes patients easier to measure urine quality at a low cost and without to go to a hospital. Each sensor has a unique ID which allows to supply single-sided access to sample under test (SUT).

The electronic circuit follows the block diagram as shown in Fig. 2 basically the electronic circuit has been designed to take several urine samples to measure pH urine, turbidity urine, and ammonia urine. All sensors are produced the different an analog voltage which the electronic circuit represents that the analog voltages are delivered to the ADC (analog-to-digital) input through the micro-controller. As a hypothesis in this study, each urine sample has a different resistor. This resistor is used as a comparison of urine content including pH, turbidity, and ammonia concentration.

All electronic circuit are implemented and assembled in the form of prototype as shown in Fig. 3. This prototype was designed using 3D CAD software to minimize the overall size of the system.

2.2. Software design

Fig. 4 shows the flowchart of our system. Once the Arduino Nano was connected to the power supply, the system automatically started initializing and reading all sensors. The Arduino Nano is constantly checking the analog values of each sensor. These values are converted into digital values.

Analog values from sensors are read 1000 times and the average value is calculated. This calculation applies to pH, NTU, and ppm. The looping systems are installed in this prototype which the system starts to work and read the sensor from $i = 0$. If the condition of i is less than 1 approximately equals to 1000, then $f = \frac{i}{1000}$ and was repeated until 1000, the read value is analog value then it was converted to pH measurement values, Nephelometric Turbidity Units (NTU), and parts per million (ppm). All results are displayed and delivered to the LCD display sensor calibration. Library "U8glib.h" was installed in the Arduino Nano as the initialization program of LCD and the initialization of the pin number for the output. The initialization program can be seen in Fig. 5.

The purpose of the initialization is to determine the variables that will be used in this sensor. For this initialization, we assigned a unique pin number to each sensor for pH, turbidity, and ammonia. Fig. 6 shows the pin for the pH sensor, turbidity sensor, ammonia sensor, the float,

```
//Initialization Program PH
cost int PH = A0;
float Po;
float data;
float VoltagePH;
float SensorPH;
```

a) Initialization pH4502C as pH sensor

```
//Initialization Program Turbidity
const int TBY = A4;
int val;
static float kekeruhan;
static float voltageTBY;
float sensorTBY;
float dataTBY;
```

b) Initialization SEN0189 as turbidity sensor

```
//Initialization Program MQ137
int MQ = A5; //Sensor pin
float m = -0.263; //Slope
float b = 0.42; //Y-Intercept
float R0 = 2.78;//Sensor Resistance in fresh air from
previous code
float voltageMQ;
float Rsgas;
float ratio;
float sensor MQ;
```

c) Initialization MQ137 as ammonia sensor

Fig. 6. Initialization three sensor, float, and integer listing: a) pH, b) Turbidity, and c) ammonia.

```
void setup()
{
 serial .begin(9600);
 u8g.seFont(u8g_font_6x10);
}
```

Fig. 7. An Initialization output analog data in LCD.

and integer variable.

According Fig. 6. The input data from each sensor are marked on the input pin: pH sensor marked on pin (A0), turbidity sensor marked on pin (A4), and ammonia sensor marked on pin (A5). The purpose of the initialization is to determine the variable that used in the sensors. The initialization in library also requires the initialization pin from pH sensor, ammonia sensor, and turbidity sensor which this is to recognize the sensor through the pin by sensor. Float variable is used to output analog data into digital numbers in the form of fractions while integer (int) is used to output the analog to an integer. Output on LCD display can use initialization "serial.begin(9600)" as shown in Fig. 7.

"serial.begin(9600)" is to determine the speed of sending and receiving data through the serial port which in the above program uses a speed of 9600 bps. U8g.sseFont(u8g_font_5x10) is to set the font that comes out on the LCD. After the initialization program is prepared according to the needs of each component and variable, the next step is to arrange the initialization program according to the system flowchart (seen Fig. 4). the reason for choosing "serial.begin(9600)" includes: the speed of sending and receiving in the system is suitable and minimal error, the baud rete "serial.begin(9600)" is the baud rate that corresponds to the data transferred between microcontroller and PC, and the standard pc in this system is 9600. These flowcharts are displayed the looping program the sequence of commands is continuously repeated until a condition is reached as shown in Fig. 8. These initializations main from three sensors are looped 1000 times. The purpose of this program is to get the steady data from sensor.

2.3. Sensor calibration

Sensor calibration is performed by matching its value to a known standard value. pH calibration was conducted by comparison utilizing pH digital measurement tool and pH liquid which is pH was calibrated by immersing pH sensor on pH liquid 4.00 and pH 6.86 to compare until the value represents similar measurement result to liquid pH metered. If measurement result hasn't been accurate yet, then the calibration voltage was changed rapidly to be adapted and wait until the measured value is equal to liquid value. Turbidity sensor (SEN0189) calibration utilizes distillation water until indicate turbidity point on 0 NTU. Whereas ammonia sensor (MQ137) was calibrated using ammonia liquid with calibration result show on 0 ppm.

2.4. Data collection

Data collections are taken from 15 urine samples with 30 ml each sample. Void urine in the morning was used in this research to know urine quality based on the first voided urine by respondent after early wake up before doing any activities. Every device and sensor are turned on and successfully carried out the testing. Then sensors were dipped to urine sample for a few minutes until the appearing value on LCD unchanged. These procedures are applied for pH test, turbidity test, and ammonia test. To keep the accuracy, measured sample was kept for data collection. The urine sample testing procedures are displayed in Fig. 8.

3. Results and discussions

In this study, first-morning-void urine was examined to know urine quality based on the first voided urine by the respondent after an early wake up before doing any activity. First-void urine was examined to know urine quality based on the first voided urine by the respondent after an early wake up before doing any activity. First-void urine is valuable to measure albuminuria and is more reliable than 24-H urine void introduced by [69]. According to [70,71] the first-void urine consists of the value of urea, calcium, urine acid, and phosphorus. Our systems are implemented to examine pH urine, turbidity urine, and ammonia urine from 15 respondents in which the result from systems have been compared with manual calculation using equation. Three sensors are included: pH4502C as pH sensor, SEN0189 as turbidity sensor, and MQ137 as ammonia sensor. The experiment results from pH detection, turbidity detection, and ammonia detection are described below:

```
void loop()
{
for(int a = 0; a < 1000; a++)
{
sensorTBY = sensorTBY + analogRead(TBY);
}
sensorMQ = analogRead(MQ);
sensorTBY = sensorTBY/1000.0;
val= sensorTBY+808;

sensorPH = sensorPH/1000.0;
double VoltagePh = sensorPH*(5.0/1023.0);
Po = 6.86 + ((2.67 - VoltagePh) / 0.17);

VoltageTBY =  val*(5.0/1023.0);
VoltageMQ = sensorMQ*(5.0/1023.0);

Turbidity = 100.00-(voltageTBY/5)*100.00;
RSgas = ((5.0*10.0)/voltageMQ)-10.0;
ratio = RS_gas/R0;
double ppm_log = (log10(rasio)-b)/m;
 double ppm = pow(10, ppm_log);
```

Fig. 8. An initialization main program of pH, turbidity, and ammonia.

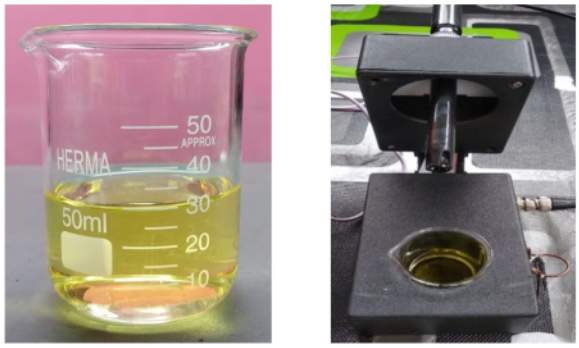

Fig. 9. Urine sampling.

3.1. pH detection on firstvoid urine

pH urine levels were used to identify the presence of disease in the body. pH sensors have been reported by [72] to detect urea in urine through the implementation of iridium oxide films (IROF). According to [73] pH normal on human urine ranging from 4.5 to 8.0. In this study, a PH4502C sensor was applied to read pH in urine that combined with Arduino Nano to convert pH value to digital analog. Then the pH value has shown at LCD Display. This system was relevant with the work from [74] in which they have applied the temperature sensor in the body by using the DS600 sensor. The sensor was designed to send the analog to digital (ADC) input of the micro-controller. A detection system representing analog value to LCD was also used by [58] to monitor heart rate using MAX30100.

In this study, human urine was obtained from 15 respondents and saved at cup/glass like as show in Fig. 9 This prototype was designed flexibly to facilitate patient on urine testing. Before test, this system previously was calibrated using buffer liquid to obtain accurate result like on Section 3. Calibration process and tools testing may affect the

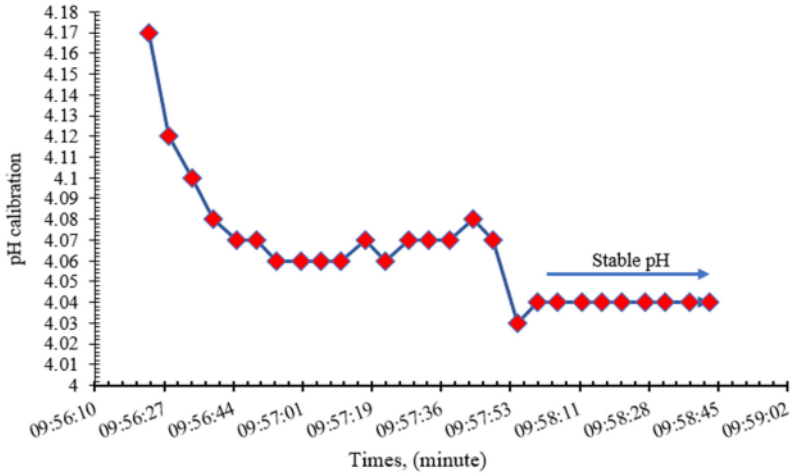

Fig. 10. The calibration process and tool testing of pH sensor.

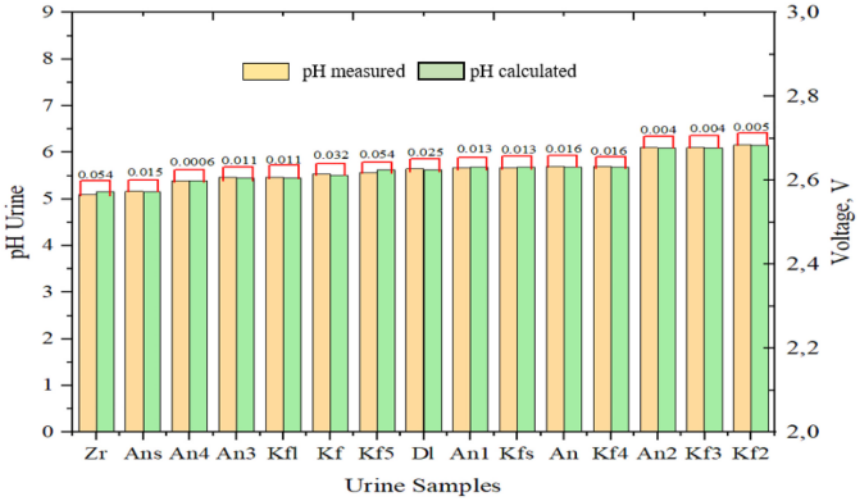

Fig. 11. The testing result of pH sensorby using prototype (pH measured), the calculation of pH urine manually (pH calculated) and voltage.

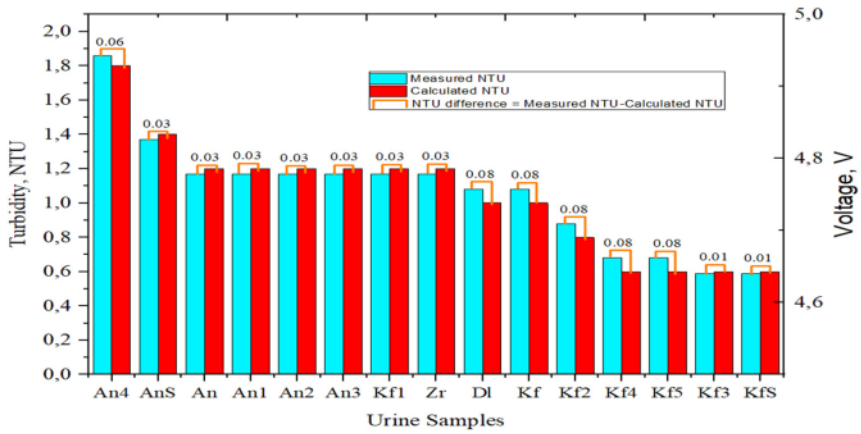

Fig. 12. The testing result of turbidity sensor by using prototype (measured pH), the calculation of pH urine manually (calculated pH) dan voltage.

rated voltage and calibration voltage which can be seen in Fig. 10.

According to Fig. 10 pH values were firstly shown around 4.17. Then pH values were reduced and stable at 4.04. These were indicated that the human urine samples were stable. Sensor calibration methods are followed for other experiments. Stable pH at calibration stage requires time around 1 min. Sensor calibrations aims to obtain appropriate result with the real condition. Every sensor previously are calibrated before testing [75]. Rated Voltage (RV) is voltage obtained by prototype. However, Calibration Voltage (CV) is voltage obtained along calibration process. Rate voltage value and calibration voltage can be utilized to count error percentage. To obtain accurate result, this tool has been compared between measured pH and pH Calculated manually which is measured pH is testing result using prototype. However, pH calculated is the result of pH calculation using Eq. (1).

$$Po = 6,86 + \frac{2,68 - 2,97}{0,17} \tag{1}$$

Where, *Po* represents pH calculated, Cv represents calibration voltage, and Rv represents rated voltage. The value of Cv is2.68. Cv value is 2.97 and pH buffer tuning is 0.17

The voltage in the sensor was displayed as the human body a large resistor [76]. The output system from microcontroller is influenced on the voltage. Furthermore, error value on this prototype was determined by using different value between measured pH and calculated pH. Error percentage values were determined using Eq. (2). The calculation of pH measured and pH calculated can be seen in Eq. (1). The result of pH calculation was indicated that this tool has difference pH measured and pH calculated relativ small. Error percentage from pH sensor was described in Eq. (2).

$$Error\ percentage = \left| \frac{pH\ measured - pH\ calculated}{pH\ calculated} \right| \times 100\% \tag{2}$$

The calculation voltage result, measured pH, and calculated pH on urine detection testing are described in Fig. 11.

pH urine detection in Fig. 11 represents the result of pH measured, pH calculated, and voltage (V). pH measured was obtained from pH testing result of urine by using prototype like as Fig. 3. However, pH calculated was obtained from manual calculation. pH measured and pH calculated aims to know the error percentage of every sample which was obtained from the difference of pH measured and pH Calculated. Form this testing, the prototype found the difference value between pH measured and pH Calculated relatively normal with a average value of pH measured was 5.6293 and pH calculated was 5.6286. The difference between the testing result of pH measured and pH calculated was around 0.0188. According to the result of this study, pH urine detection from respondents indicates the normal level. Voltage can be used to identify the pH urine. The voltage from systems is indicated an increase when the pH increases. Voltage as a resistor for the object like body, urine, and blood. The output result from the sensor is influenced by voltage introduced by [66]. As a resistor, the voltage also uses in the field of agriculture to measure nitrogen in the paddy soil over the TCS3200 sensor to identify the color [77]. The voltage sensor can be determined the AC or DC voltage level. The type of voltage is resistive type sensor and capacitor type. From these study, the pH urine and voltage have a straight proportional. In addition, voltage in the systems are affected by pH urine. When the pH urine is high level, such as the respondent's urine (kf2), the voltage value also increases. It means that human urine has different resistance. Moreover, urine resistance can be used as a particular parameter for pH measurement. According to [76,78] sensor detection in human urine depends on the voltage output divider equation which every human urine has a different resistor. Several previous study from [59,60] have reported that the diagnosis smart sensing to detect creatinine level using a sensor is depended on voltage output on creatinine. Voltage output from sensor also can be used to measure heart rate, skin temperature dan galvanic skin using the sensor. The respondent in this study has a different resistance. As a basic line, the result of pH urine detection was dependent on the result of output voltage. The detail can be seen in Fig. 11. The higher the voltage generated, the pH in the urine is more alkaline and increases. This result was relevant to the previous research from [80] that pH measurement depends on the output voltage. This prototype has been calculated the error percentage to validate the tool. This tool was proved to be able to measure pH urine with an error percentage of 0.0061% (very small). The highest pH level from 15 respondents are urine from kf2 and the lowest pH urine from respondents are code (zr). 15 respondents in this study were indicated that there were no symptoms of diabetes and the pH measurement results from respondents were declared normal. According to [79] normal values for urine is ranging from pH 5.0 to 6.0.

3.2. Turbidity detection on first-void urine

Before urine was tested, this tool previously was calibrated using distillation water until the turbidity point is 0 NTU. Then 15 urine samples were tested using a turbidity sensor to know the turbidity of urine.Urine solubility signal can be used to detect deposition of protein albumin and globulin on urine. Provious research from [78] discussed that the measurement of turbidity urine is measured through continuity flow principle using an infrared sensor. However, this study was installed sensor turbidity directly in the sample urine. According to [69]

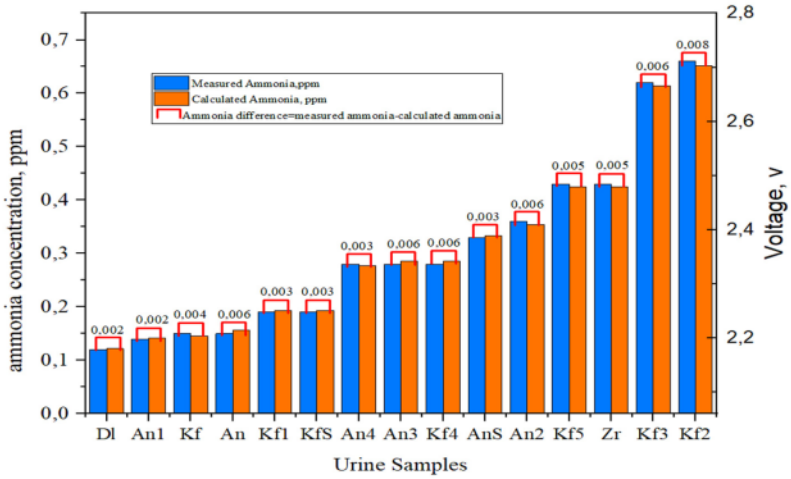

Fig. 13. The testing result of ammonia sensor by using prototype (measured pH), the calculation of pH urine manually (calculated pH) dan voltage.

turbid urine indicate that human urine has the deposition of protein albumin and globulin, while clear urine indicates healthy urine. The turbidity sensor is a device for reading the level of turbidity in a liquid with NTU (Nephelometric Turbidity Units). The workings of this sensors are the light emitted into the liquid will be blocked by particles and deposits suspended then the level of scattering and transmitted light will be received by the photodiode and measured. SEN0198 as turbidity sensor was applied to measure the turbidity urine which this prototype was developed by using EPA Method 180.1 [85]. As validation section, it is observed that the EPA Method 180.1 is suitable for measuring the turbidity levels from 0 to 40 NTU (nephelometric turbidity units). These systems are relatively complex. However, the EPA Method 180.1 is not able to measure at turbidity levels above 40 NTU. as the equation based on instruments in compliance with the EPA Method 180.1 are suitable for measuring turbidity, the formula for NTU can be seen in Eq. (3).

$$NTU = \left(\frac{A \times (B + C)}{C}\right) \tag{3}$$

Where, A is NTU found in diluted sample, B is volume of dilution water, mL, and C is sample volume taken for dilution, mL. In a single laboratory (EMSL-Cincinnati), using surface water samples at levels of 26, 41, 75, and 180 NTU, the standard deviations were ±0.60, ±0.94, ±1.2, and ±4.7 units, respectively. The experiment result shown that the measured NTU from system or prototype was compared with calculated NTU from manual calculation using by using Eq. (4). The purpose of this comparison is to know the error percentage of this tool. Urine from 15 respondents has been taken in the morning to be tested those turbidity rates.

$$error\ percentage = \left|\frac{turbidity\ measured - turbidity\ calculated}{turbidity\ calculated}\right| \times 100\% \tag{4}$$

In detail, turbidity testing result using prototype, manual calculation, and voltage can be seen in this Fig. 12 below:

As Fig. 12. it shows that the voltage also was affected by turbidity value from urine sample. The correlation between turbidity measured and turbidity calculated were simulation by using the coefficient of determination (R^2) with significant correlation that can be seen in Fig. 14. Sample urine with code (An4) indicates high turbidity level and high voltage. While sample urine with code (KfS) indicates low turbidity level and low voltage. When the voltage test tool increases then the turbidity rate also increases. Output turbidity value of urine was dependent on output voltage urine in which human urine has a different resistor. This result was in line with the review of [82] that the voltage comparison with TSS concentration is directly proportional, in which the higher TSS concentrate, the higher voltage result. Furthermore, the experiment result shows that the measured NTU is value from the system or prototype with average result of 0.59 NTU while the calculated NTU is manual calculation using Eq. (4).with the average result of 0.60 NTU. The average of error percentage from these calculations are 5.098% (very small). These results are indicated that the tool was proved to be able to measure turbidity in human urine.

3.3. Ammonia concentration detection on first-morning-void urine

The sensor was applied to detect ammonia concentration in urine using MQ137 that was calibrated by using ammonia liquid. The MQ-137 sensor is an electrochemical sensor and varies resistance to ammonia gas (NH_3). The workings of this sensors are to use a heater contained in the sensor section when exposed to ammonia gas (NH_3), the value of the resistance of the sensor will change. The urine testing was applied in the morning to know urine quality like as explained in Section 1. Ammonia concentration in urine was used for the first detection of diseases like kidney, urinary tract disorders, and gastrointestinal bleeding [76]. The use of ammonia sensors may decrease cost, more flexible and disposable sensing platform that can be validated easier [78]. These systems were installed the current output of 0-4 vdc signal with a 220 Ω resistor which ADC system was transferred to Arduino as digital converter. As formula, these systems can be calculated by using Eq. (5)..

$$V = \left(\frac{A}{1023}\right) \times 5 \tag{5}$$

Where, V is voltage, Vdc, A is digital count, 5 is full scale ADC voltage range, and 1023 is 2^{10}-1 as number of discrete counts for 10-bit ADC. According Eq 4 can be used to calculate the resistance error of the sensor. The result of ammonia concentration of urine in this prototype was compared with manual calculation to know the error percentage of these tools. The manual calculation of urine ammonia concentrate was used in Eq. (6).

… The equation of resistance error (RS) can be used for any gas

$$R_s = \frac{5 \times R_S}{V} \times R_L \tag{6}$$

Where V is voltage and R_L *is* resistance load of the MQ137 sensor. After resistance error was obtained, then be calculated ratio between RS_{gas}

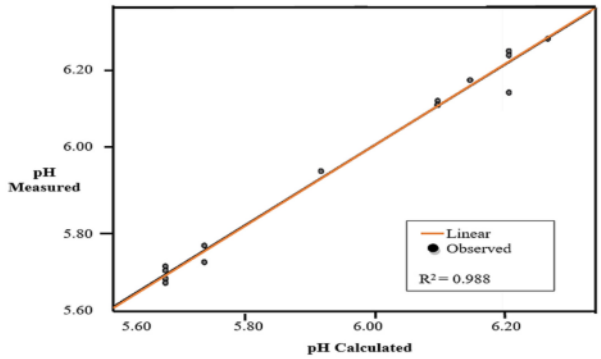

a) The correlation between pH measured and pH calculated

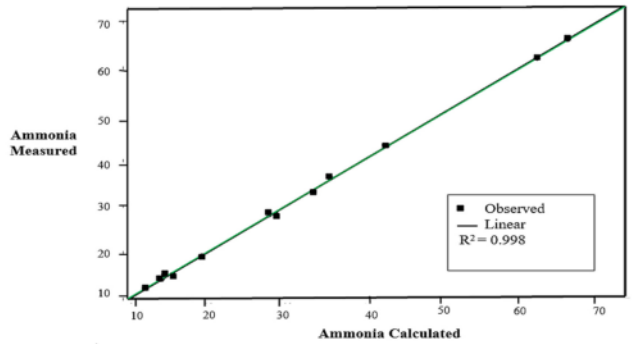

b) The correlation between ammonia measured and ammonia calculated

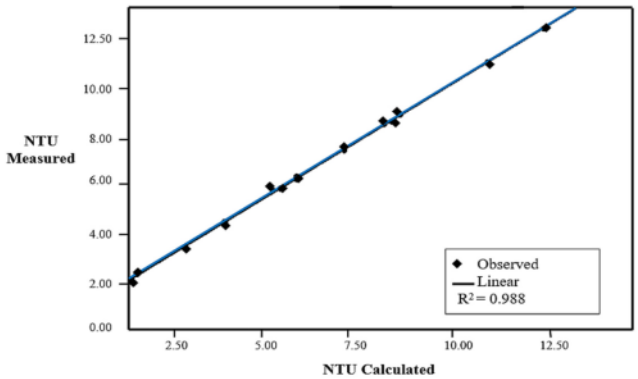

c) The correlation between turbidity measured and turbidity calculated

Fig. 14. The correlation test between sensor measured (pH, ammonia, and turbidity) and sensor calculated.

and *RO* using in Eq. (7).

.

$$Ratio = \frac{R_{S_{gas}}}{RO} \tag{7}$$

To look for difference value of pp, between measured ammonia and calculated ammonia are described in Eq. (8)..

$$error\ percentage = \left|\frac{ppm\ measured - ppm\ calculated}{ppm\ calculated}\right| \times 100\% \tag{8}$$

The experiment result from ammonia concentration using this system are included manual calculation of ammonia concentration, and voltage that shown in Fig. 13.

As Fig. 13. It shows that the correlation between measured ammonia (using a prototype) and calculated ammonia (using an equation) was affected by voltage. The ammonia concentration is straight proportional where ammonia concentration is low then the voltage is also low. Sample urine with code (Kf2) indicates high ammonia level and high voltage value while sample urine with code (Dl) indicates low ammonia level and low voltage value. These systems are applied in 15 urine samples to identify the ammonia in urine. Voltage in this system can be used to identify ammonia concentration in urine because every urine has

a different resistor. This work was relevant to the previous research from [80] which reported the ammonia sensor for health monitoring with the result of the increasing of current based on the ammonia concentration. When the current was increased, the ammonia concentration was increased also. Other research has investigated the effect currently on urine detection [81] and blood cells in urine [82]. the voltage output changes in proportion to the time of testing carried out. The sensor of this prototype can read ammonia concentrate in urine. Based on the experiment results, the error percentage from this system is very small with an average of 1.679%. The average of the measured ammonia from the system or prototype is 0.66 ppm while the average of the calculated ammonia from manual calculation using equation is 0.65 ppm. From the experiment result, the measurement of the ammonia concentration from 15 respondents are indicated that the respondents are declared under normal conditions. These results have been compared with the results of a study from [83] which reported that chronic kidney disease (CKD) patients had ammonia levels ranging from 1.26 to 6.33 ppm. This system was proved to be able to measure the ammonia concentration in human urine.

3.4. Sensor accuracy

The correlation between sensor measured value from the prototype and sensor calculated value from the equation applies to identify the sensor accuracy. The coefficient of determination (R^2) quantifies the amount of variability on the dependence variable was described by the model in Eq. (9)

$$R^2 = \frac{SST}{SSE} - 1 \tag{9}$$

Where SSE represents the sum of squared errors (squared residuals). SST represents the sum of squared variation on a dependent variable. The regression models have refined the analysis through the coefficient of determination R-squared (R^2) values which is the range of R-squared between 0% and 100%. The higher R-squared (R^2) represents a higher explanation of the response data. In addition, the statistical analysis to know the significant difference between sensor measured value and sensor calculated value can be performed by using *p*-value (Chi-square test). *P*-value is one analysis of non-parametric comparative test that conducted on two variables (independency test) where the data scale of both variables is nominal. P-value can be described by using in Eq. (10).

$$x^2 = \Sigma \frac{(0i - Ei)^2}{Ei} \tag{10}$$

Where, X^2 represents Chi square value, $0i$ represents observed value, and Ei represents expected value.

The experiment result found that R^2 value from pH sensor, ammonia sensor, and turbidity sensor are 0.968, 0.998, and 0.988 respectively. These data are indicated that the correlation between sensor measured and calculated is significant. The accuracy from each sensor (pH, ammonia, and turbidity) are 97.693%, 98.321%, and 97.095%. In addition, p-value analysis from this prototype is 0.166 of pH sensor, 0.009 of ammonia sensor, and 0.250 of turbidity sensor. From each sensor, *p*-values are greater than 0.001 (level of significance) which it describes that the difference between sensor measured and sensor calculated is no significant difference. P-value can be described in Fig. 14 which the correlation from the analysis is linear. In other word, the output of the prototype is acceptable value. These results are relevant with the previous research from [82] that are applied to find the correlation between the actual and measured volume of urinary with the accuracy is 95.51% and the correlation between actual from prototype and measured volume is linear characteristic.

4. Conclusions

Three sensors are applied in this study to create a urine quality detector consisting of pH urine, turbidity urine, and ammonia urine using multi sensor. The sensors consisted of: pH4502C as pH sensor, turbidity sensor, and MQ-137 as ammonia sensor. The study was carried out non-inventively by collecting urine samples from 15 healthy subjects or respondents. The experiment results were indicated that the average of the error percentage from pH sensor, turbidity sensor, and ammonia sensor were of 0.0061% (very small), 5.098% (very small), and 1.679% (very small). In addition, the pH level, turbidity, and ammonia concentration were affected by voltage which the increasing of pH, turbidity, and ammonia concentration in human urine was proportional with the increasing of voltage in the system or prototype. From the experiment result, the measurement of pH, turbidity, and ammonia concentration from 15 respondents were indicated that the respondents were declared under normal condition and not found any disease like diabetes. The accuracy of pH sensor, ammonia sensor, and turbidity sensor are 97.693%, 98.321%, and 97.095%.

Declaration of Competing Interest

The authors have stated no conflict of interest.

Acknowledgement

This research project was supported by Kemendikbud-Ristek Republic of Indonesia with contract number of 311/E4.1/AK.04.PT/2021.

References

[1] S. Bouatra, et al., The human urine metabolome, PLoS One 8 (9) (2013), https://doi.org/10.1371/journal.pone.0073076.
[2] J. Bernard, L. Song, B. Henderson, G.E. Tasian, Association between daily water intake and 24-hour urine volume among adolescents with kidney stones, Urology 140 (2020) 150–154, https://doi.org/10.1016/j.urology.2020.01.024.
[3] C. Mir, et al., Analysis of urine composition from split 24-h samples: use of 12-h overnight samples to evaluate risk factors for calcium stones in healthy and stone-forming children, J. Pediatr. Urol. 16 (3) (2020) 371.e1–371.e7, https://doi.org/10.1016/j.jpurol.2020.02.011.
[4] I. Yaroshenko, D. Kirsanov, L. Kartsova, A. Sidorova, I. Borisova, A. Legin, Determination of urine ionic composition with potentiometric multisensor system, Talanta 131 (2015) 556–561, https://doi.org/10.1016/j.talanta.2014.08.030.
[5] P.J. McIntire, I. Kilic, E.M. Wojcik, G.A. Barkan, S.E. Pambuccian, The color of urine: then and now—a comprehensive review of the literature with emphasis on intracytoplasmic pigments encountered in urinary cytology, J. Am. Soc. Cytopathol. 9 (1) (2020) 9–19, https://doi.org/10.1016/j.jasc.2019.05.002.
[6] R.D. Aycock, D.A. Kass, Abnormal urine color, South. Med. J. 105 (1) (2012) 43–47, https://doi.org/10.1097/SMJ.0b013e31823c413e.
[7] C.O. Asogwa, S.F. Collins, P. McLaughlin, D.T.H. Lai, A galvanic coupling method for assessing hydration rates, Electron. 5 (3) (2016) 1–16, https://doi.org/10.3390/electronics5030039.
[8] C.I.B. Vela, F.J.B. Padilla, Determination of ammonia concentrations in cirrhosis patients-still confusing after all these years? Ann. Hepatol. 10 (Suppl. 2) (2011) S60–S65, https://doi.org/10.1016/s1665-2681(19)31609-6.
[9] M.M. Adeva, G. Souto, N. Blanco, C. Donapetry, Ammonium metabolism in humans, Metabolism. 61 (11) (2012) 1495–1511, https://doi.org/10.1016/j.metabol.2012.07.007.
[10] T.L. Chipako, D.G. Randall, Urine treatment technologies and the importance of pH, J. Environ. Chem. Eng. 8 (1) (2020) 103622, https://doi.org/10.1016/j.jece.2019.103622.
[11] W. Tao, A. Bayrakdar, Y. Wang, F. Agyeman, Three-stage treatment for nitrogen and phosphorus recovery from human urine: hydrolysis, precipitation and vacuum stripping, J. Environ. Manage. 249 (July) (2019) 109435, https://doi.org/10.1016/j.jenvman.2019.109435.
[12] M. Vallet, et al., Urinary ammonia and long-term outcomes in chronic kidney disease, Kidney Int. 88 (1) (2015) 137–145, https://doi.org/10.1038/ki.2015.52.
[13] A.C. Simões e Silva, E.A. Oliveira, R.H. Mak, Urinary tract infection in pediatrics: an overview, J. Pediatr. (Rio. J) 96 (2020) 65–79, https://doi.org/10.1016/j.jped.2019.10.006.
[14] J.K. Byron, Urinary tract infection, Vet. Clin. North Am. - Small Anim. Pract. 49 (2) (2019) 211–221, https://doi.org/10.1016/j.cvsm.2018.11.005.
[15] H. Iwasaki, T. Shimura, H. Kataoka, Current status of urinary diagnostic biomarkers for colorectal cancer, Clin. Chim. Acta 498 (July) (2019) 76–83, https://doi.org/10.1016/j.cca.2019.08.011.

[16] C. Magagnotti, et al., Identification of nephropathy predictors in urine from children with a recent diagnosis of type 1 diabetes, J. Proteomics 193 (June 2018) (2019) 205–216, https://doi.org/10.1016/j.jprot.2018.10.010.
[17] C. Qiu, et al., Early pregnancy urinary biomarkers of fatty acid and carbohydrate metabolism in pregnancies complicated by gestational diabetes, Diabetes Res. Clin. Pract. 104 (3) (2014) 393–400, https://doi.org/10.1016/j.diabres.2014.03.001.
[18] B. Sun, et al., Urinary biomarker evaluation for early detection of gentamycin-induced acute kidney injury, Toxicol. Lett. 300 (August 2018) (2019) 73–80, https://doi.org/10.1016/j.toxlet.2018.10.027.
[19] A.E. Omer, et al., Low-cost portable microwave sensor for non-invasive monitoring of blood glucose level: novel design utilizing a four-cell CSRR hexagonal configuration, Sci. Rep. 10 (1) (2020) 1–20, https://doi.org/10.1038/s41598-020-72114-3.
[20] M.S. Islam, Fasting blood glucose and diagnosis of type 2 diabetes, Diabetes Res. Clin. Pract. 91 (1) (2011) 8227, https://doi.org/10.1016/j.diabres.2010.09.035.
[21] S. Bisht, S.S. Sisodia, P. Mahendra, N. Sharma, Oral glucose tolerance test: an essential tool to make the diagnosis of diabetes, Int. J. Pharm. Sci. Rev. Res. 6 (2) (2011) 48–55.
[22] S.I. Sherwani, H.A. Khan, A. Ekhzaimy, A. Masood, M.K. Sakharkar, Significance of HbA1c test in diagnosis and prognosis of diabetic patients, Biomark. Insights 11 (2016) 95–104, https://doi.org/10.4137/Bmi.s38440.
[23] D.S. Ross, et al., 2016 American Thyroid Association guidelines for diagnosis and management of hyperthyroidism and other causes of thyrotoxicosis, Thyroid 26 (10) (2016) 1343–1421, https://doi.org/10.1089/thy.2016.0229.
[24] M. Srikanth, G.V. Rao, K.R.S.S. Rao, Modified assay procedure for the estimation of serum glucose using microwell reader, Indian J. Clin. Biochem. 19 (1) (2004) 34–35, https://doi.org/10.1007/BF02872385.
[25] K.S. Raj, Thyroid function tests and its interpretation, J. Pathol. Nepal 4 (7) (2014) 584–590, https://doi.org/10.3126/jpn.v4i7.10318.
[26] T. Kuhara, M. Ohse, Y. Inoue, A.J.L. Cooper, A GC/MS-based metabolomic approach for diagnosing citrin deficiency, Anal. Bioanal. Chem. 400 (7) (2011) 1881–1894, https://doi.org/10.1007/s00216-011-4766-0.
[27] S. Hussain, M. Chand Jamali, A. Habib, M.S. Hussain, M. Akhtar, A.K. Najmi, Diabetic kidney disease: an overview of prevalence, risk factors, and biomarkers, Clin. Epidemiol. Glob. Heal. 9 (May 2020) (2021) 2–6, https://doi.org/10.1016/j.cegh.2020.05.016.
[28] S. Vijay, A. Hamide, G.P. Senthilkumar, V. Mehalingam, Utility of urinary biomarkers as a diagnostic tool for early diabetic nephropathy in patients with type 2 diabetes mellitus, Diabetes Metab. Syndr. Clin. Res. Rev. 12 (5) (2018) 649–652, https://doi.org/10.1016/j.dsx.2018.04.017.
[29] W.K. Han, et al., Urinary biomarkers in the early diagnosis of acute kidney injury, Kidney Int. 73 (7) (2008) 863–869, https://doi.org/10.1038/sj.ki.5002715.
[30] A. Roointan, Y. Gheisari, K.L. Hudkins, A. Gholaminejad, Non-invasive metabolic biomarkers for early diagnosis of diabetic nephropathy: meta-analysis of profiling metabolomics studies, Nutr. Metab. Cardiovasc. Dis. 31 (8) (2021) 2253–2272, https://doi.org/10.1016/j.numecd.2021.04.021.
[31] J.-W. Wang, C.-C. Zhao, J.-F. Ke, Y. Liu, L.-X. Li, Comparison of urine uric acid excretion between type 1 and type 2 diabetes, Obes. Med. 24 (February) (2021) 100335, https://doi.org/10.1016/j.obmed.2021.100335.
[32] J. Upadhyay, et al., Pharmacotherapy of type 2 diabetes: an update, Metabolism. 78 (2018) 13–42, https://doi.org/10.1016/j.metabol.2017.08.010.
[33] S.Y. Tan, et al., Type 1 and 2 diabetes mellitus: a review on current treatment approach and gene therapy as potential intervention, Diabetes Metab. Syndr. Clin. Res. Rev. 13 (1) (2019) 364–372, https://doi.org/10.1016/j.dsx.2018.10.008.
[34] E. Buttermore, V. Campanella, R. Priefer, Diabetes & metabolic syndrome: clinical research & reviews the increasing trend of Type 2 diabetes in youth: an overview, Diabetes Metab. Syndr. Clin. Res. Rev. 15 (5) (2021) 102253, https://doi.org/10.1016/j.dsx.2021.102253.
[35] B.B. Misra, A. Misra, The chemical exposome of type 2 diabetes mellitus: opportunities and challenges in the omics era, Diabetes Metab. Syndr. Clin. Res. Rev. 14 (1) (2020) 23–38, https://doi.org/10.1016/j.dsx.2019.12.001.
[36] G.J. Becker, G. Garigali, G.B. Fogazzi, Advances in urine microscopy, Am. J. Kidney Dis. 67 (6) (2016) 954–964, https://doi.org/10.1053/j.ajkd.2015.11.011.
[37] F.D. Ince, H.Y. Ellidağ, M. Koseoğlu, N. Şimşek, H. Yalçin, M.O. Zengin, The comparison of automated urine analyzers with manual microscopic examination for urinalysis automated urine analyzers and manual urinalysis, Pract. Lab. Med. 5 (2016) 14–20, https://doi.org/10.1016/j.plabm.2016.03.002.
[38] P. Tantisaranon, K. Dumkengkhachornwong, P. Aiadsakun, A. Hnoonual, A comparison of automated urine analyzers cobas 6500, UN 3000-111b and iRICELL 3000 with manual microscopic urinalysis, Pract. Lab. Med. 24 (January) (2021) e00203, https://doi.org/10.1016/j.plabm.2021.e00203.
[39] K. Suhail, D. Brindha, A review on various methods for recognition of urine particles using digital microscopic images of urine sediments, Biomed. Signal Process. Control 68 (May) (2021) 102806, https://doi.org/10.1016/j.bspc.2021.102806.
[40] G.B. Fogazzi, J. Delanghe, Microscopic examination of urine sediment: phase contrast versus bright field, Clin. Chim. Acta 487 (July) (2018) 168–173, https://doi.org/10.1016/j.cca.2018.09.036.
[41] E.V. Karpova, E.E. Karyakina, A.A. Karyakin, Wearable non-invasive monitors of diabetes and hypoxia through continuous analysis of sweat, Talanta 215 (March) (2020) 120922, https://doi.org/10.1016/j.talanta.2020.120922.
[42] M. Bhatia, S. Kaur, S.K. Sood, V. Behal, Internet of things-inspired healthcare system for urine-based diabetes prediction, Artif. Intell. Med. 107 (July 2019) (2020) 101913, https://doi.org/10.1016/j.artmed.2020.101913.
[43] J. Guo, Smartphone-powered electrochemical dongle for point-of-care monitoring of blood β-ketone, Anal. Chem. 89 (17) (2017) 8609–8613, https://doi.org/10.1021/acs.analchem.7b02531.
[44] J. Guo, Uric acid monitoring with a smartphone as the electrochemical analyzer, Anal. Chem. 88 (24) (2016) 11986–11989, https://doi.org/10.1021/acs.analchem.6b04345.
[45] N.U. Khan, et al., Insights into predicting diabetic nephropathy using urinary biomarkers, Biochim. Biophys. Acta - Proteins Proteomics 1868 (10) (2020) 140475, https://doi.org/10.1016/j.bbapap.2020.140475.
[46] T. Majtner, E.S. Nadimi, K.B. Yderstræde, V. Blanes-Vidal, Non-invasive detection of diabetic complications via pattern analysis of temporal facial colour variations, Comput. Methods Programs Biomed. 196 (2020), https://doi.org/10.1016/j.cmpb.2020.105619.
[47] E.F.O. Kern, P. Erhard, W. Sun, S. Genuth, M.F. Weiss, Early urinary markers of diabetic kidney disease: a nested case-control study from the diabetes control and complications trial (DCCT), Am. J. Kidney Dis. 55 (5) (2010) 824–834, https://doi.org/10.1053/j.ajkd.2009.11.009.
[48] F. Waanders, G. Navis, H. van Goor, Urinary tubular biomarkers of kidney damage: potential value in clinical practice, Am. J. Kidney Dis. 55 (5) (2010) 813–816, https://doi.org/10.1053/j.ajkd.2010.02.002.
[49] V. K, D.C. Bob Zhang, Non-invasive diabetes mellitus detection using facial block color, Int. J. Recent Technol. Eng. 7 (4) (2019) 304–306.
[50] N.S. Nguyen, G. Das, H.H. Yoon, Nickel/cobalt oxide-decorated 3D graphene nanocomposite electrode for enhanced electrochemical detection of urea, Biosens. Bioelectron. 77 (2016) 372–377, https://doi.org/10.1016/j.bios.2015.09.046.
[51] A. Salek-Maghsoudi, et al., Recent advances in biosensor technology in assessment of early diabetes biomarkers, Biosens. Bioelectron. 99 (May 2017) (2018) 122–135, https://doi.org/10.1016/j.bios.2017.07.047.
[52] M.S. Kumar, S. Ghosh, S. Nayak, A.P. Das, Recent advances in biosensor based diagnosis of urinary tract infection, Biosens. Bioelectron. 80 (2016) 497–510, https://doi.org/10.1016/j.bios.2016.02.023.
[53] J. Jiang, et al., Smartphone based portable bacteria pre-concentrating microfluidic sensor and impedance sensing system, Sensors Actuators B Chem. 193 (2014) (2014) 653–659, https://doi.org/10.1016/j.snb.2013.11.103.
[54] Z. Altintas, M. Akgun, G. Kokturk, Y. Uludag, A fully automated microfluidic-based electrochemical sensor for real-time bacteria detection, Biosens. Bioelectron. 100 (September 2017) (2018) 541–548, https://doi.org/10.1016/j.bios.2017.09.046.
[55] P. Ghosh, D. Bhattacharjee, M. Nasipuri, Intelligent toilet system for non-invasive estimation of blood-sugar level from urine, IRBM 41 (2) (2020) 94–105, https://doi.org/10.1016/j.irbm.2019.10.005.
[56] T. Schlebusch, W. Fichtner, M. Mertig, S. Leonhardt, Unobtrusive and comprehensive health screening using an intelligent toilet system, Biomed. Tech. 60 (1) (2015) 17–29, https://doi.org/10.1515/bmt-2013-0140.
[57] P. Choden, T. Seesaard, U. Dorji, C. Sriphrapradang, T. Kerdcharoen, Urine odor detection by electronic nose for smart toilet application, in: *ECTI-CON* 2017 - *2017 14th Int. Conf. Electr. Eng. Comput. Telecommun. Inf. Technol*, 2017, pp. 190–193, https://doi.org/10.1109/ECTICon.2017.8096205.
[58] S. Al Irfan, A. Yudhana, S.C. Mukhopadhyay, I.R. Karas, D.E. Wati, I. Puspitasari, Wireless communication system for monitoring heart rate in the detection and intervention of emotional regulation, in: *Proc. - 1st Int. Conf. Informatics, Multimedia, Cyber Inf. Syst. ICIMCIS* 2019, 2019, pp. 243–248, https://doi.org/10.1109/ICIMCIS48181.2019.8985210.
[59] B. Chen, C.Q. Pan, Non-invasive assessment of fibrosis and steatosis in pediatric non-alcoholic fatty liver disease, Clin. Res. Hepatol. Gastroenterol. (2021) 101755, https://doi.org/10.1016/j.clinre.2021.101755.
[60] Y. Gao, et al., An interrelated CataFlower enzyme system for sensitively monitoring sweat glucose, Talanta (2021) 122799, https://doi.org/10.1016/j.talanta.2021.122799.
[61] S.N. Prabhu, S.C. Mukhopadhyay, C. Gooneratne, A.S. Davidson, G. Liu, Interdigital sensing system for detection of levels of creatinine from the samples, Proc. Int. Conf. Sens. Technol. ICST 2019-Decem (2019) 2–7, https://doi.org/10.1109/ICST46873.2019.9047672.
[62] S. Prabhu, C. Gooneratne, K. Anh Hoang, S. Mukhopadhyay, Development of a Point-of-Care diagnostic smart sensing system to detect creatinine levels, Midwest Symp. Circuits Syst. 2020-Augus (2020) 77–80, https://doi.org/10.1109/MWSCAS48704.2020.9184441.
[63] S. Nitin Prabhu, C.P. Gooneratne, K.-A. Hoang, S.C. Mukhopadhyay, IoT-associated Impedimetric biosensing for point-of-care monitoring of kidney health, IEEE Sensors J. 21 (13) (2020) 14320–14329, https://doi.org/10.1109/jsen.2020.3011848.
[64] N. Promphet, S. Ummartyotin, W. Ngeontae, P. Puthongkham, N. Rodthongkum, Non-invasive wearable chemical sensors in real-life applications, Anal. Chim. Acta (xxxx) (2021) 338643, https://doi.org/10.1016/j.aca.2021.338643.
[65] A. Yudhana, R. Umar, F.M. Ayudewi, The monitoring of corn sprouts growth using the region growing methods, J. Phys. Conf. Ser. 1373 (1) (2019), https://doi.org/10.1088/1742-6596/1373/1/012054.
[66] A. Yudhana, J. Rahmayanti, S.A. Akbar, S. Mukhopadhyay, I.R. Karas, Modification of manual raindrops type observatory ombrometer with ultrasonic sensor HC-SR04, Int. J. Adv. Comput. Sci. Appl. 10 (12) (2019) 277–281, https://doi.org/10.14569/ijacsa.2019.0101238.
[67] A. Yudhana, A. Muslim, D.E. Wati, I. Puspitasari, A. Azhari, M.M. Mardhia, Human emotion recognition based on EEG signal using fast fourier transform and K-Nearest neighbor, Adv. Sci. Technol. Eng. Syst. 5 (6) (2020) 1082–1088, https://doi.org/10.25046/aj0506131.

[68] S.C. Mukhopadhyay, G. Sen Gupta, A physiological parameter monitoring device to care for the elderly, in: Proc. IEEE Sensors, 2008, pp. 1324–1327, https://doi.org/10.1109/ICSENS.2008.4716689.
[69] X. Liu, et al., Which is the urine sample material of choice for metabolomics-driven biomarker studies? Anal. Chim. Acta 1105 (2020) 120–127, https://doi.org/10.1016/j.aca.2020.01.028.
[70] J. Pattyn, et al., Human papillomavirus detection in urine: Effect of a first-void urine collection device and timing of collection, J. Virol. Methods 264 (June 2018) (2019) 23–30, https://doi.org/10.1016/j.jviromet.2018.11.008.
[71] C. Gys, M. Bastiaensen, G. Malarvannan, Y. Ait Bamai, A. Araki, A. Covaci, Short-term variability of bisphenols in spot, morning void and 24-hour urine samples, Environ. Pollut. 268 (2021) 115747, https://doi.org/10.1016/j.envpol.2020.115747.
[72] E. Prats-Alfonso, L. Abad, N. Casañ-Pastor, J. Gonzalo-Ruiz, E. Baldrich, Iridium oxide pH sensor for biomedical applications. Case urea-urease in real urine samples, Biosens. Bioelectron. 39 (1) (2013) 163–169, https://doi.org/10.1016/j.bios.2012.07.022.
[73] J. Liu, et al., Integrated hand-held electrochemical sensor for multicomponent detection in urine, Biosens. Bioelectron. 193 (May) (2021) 113534, https://doi.org/10.1016/j.bios.2021.113534.
[74] K. Malhi, S.C. Mukhopadhyay, J. Schnepper, M. Haefke, H. Ewald, A zigbee-based wearable physiological parameters monitoring system, IEEE Sensors J. 12 (3) (2012) 423–430, https://doi.org/10.1109/JSEN.2010.2091719.
[75] S. Aitekenov, A. Gaipov, R. Bukasov, Review: detection and quantification of proteins in human urine, Talanta 223 (P1) (2021) 121718, https://doi.org/10.1016/j.talanta.2020.121718.
[76] N.K. Suryadevara, S.C. Mukhopadhyay, L. Barrack, Towards a smart non-invasive fluid loss measurement system, J. Med. Syst. 39 (4) (2015), https://doi.org/10.1007/s10916-015-0206-6.
[77] A. Yudhana, D. Sulistyo, I. Mufandi, GIS-based and Naïve Bayes for nitrogen soil mapping in Lendah, Indonesia, Sens. Bio-Sensing Res. 33 (2021) 100435, https://doi.org/10.1016/j.sbsr.2021.100435.
[78] W. Wu, H. Zhang, S. Pirbhulal, S.C. Mukhopadhyay, Y. Zhang, Physiological monitoring system, IEEE Sensors J. 15 (12) (2015) 7087–7095.
[79] X. Zhang, et al., Detection of biomarkers in body fluids using bioprobes based on aggregation-induced emission fluorogens, Mater. Chem. Front. 4 (9) (2020) 2548–2570, https://doi.org/10.1039/d0qm00376j.
[80] K. Rithin Paul Reddy, S.S. Srija, R. Karthi, P. Geetha, Evaluation of water body extraction from satellite images using open-source tools, in: 4th International Symposium on Intelligent Systems Technologies and Applications, ISTA 2018 vol. 910, Springer Verlag, Department of Computer Science and Engineering, Amrita School of Engineering, Amrita Vishwa Vidyapeetham, Coimbatore, India, 2020, pp. 129–140, https://doi.org/10.1007/978-981-13-6095-4_10.
[81] W. Huang, et al., Turbidimeter design and analysis: a review on optical fiber sensors for the measurement of water turbidity, Sensors Actuators, B Chem. 88 (July) (2018) 124187, https://doi.org/10.1016/j.snb.2021.130621.
[82] M.V.C. Padilla, F.R.G. Cruz, A monitoring device for urine volume and turbidity using continuity flow and beer- Lambert's Law for post-operative patients, in: 2019 IEEE 11th Int. Conf. Humanoid, Nanotechnology, Inf. Technol. Commun. Control. Environ. Manag. HNICEM 2019, 2019, pp. 1–6, https://doi.org/10.1109/HNICEM48295.2019.9072770.
[83] A.F. Bin Omar, M.Z. Bin MatJafri, Turbidimeter design and analysis: a review on optical fiber sensors for the measurement of water turbidity, Sensors 9 (10) (2009) 8311–8335, https://doi.org/10.3390/s91008311.
[85] James W O'Dell. METHOD 180.1 - DETERMINATION OF TURBIDITY BY NEPHELOMETR, William Andrew Publishing, Westwood, NJ, 1886, pp. 378–387, https://doi.org/10.1016/B978-0-8155-1398-8.50021-5. Submitted for publication.

HASIL CEK9_60010383

ORIGINALITY REPORT

10%	9%	3%	1%
SIMILARITY INDEX	INTERNET SOURCES	PUBLICATIONS	STUDENT PAPERS

PRIMARY SOURCES

1	www.x-mol.com Internet Source	6%
2	Sixolile Centane, Sithi Mgidlana, Yolanda Openda, Tebello Nyokong. "Electrochemical detection of human epidermal growth factor receptor 2 using an aptamer on cobalt phthalocyanines – Cerium oxide nanoparticle conjugate", Bioelectrochemistry, 2022 Publication	1%
3	Submitted to University of Leicester Student Paper	1%
4	www.fondriest.com Internet Source	1%
5	ouci.dntb.gov.ua Internet Source	1%
6	docplayer.net Internet Source	1%

Exclude quotes	On	Exclude matches	< 1%
Exclude bibliography	On		